ORIGINAL ARTICLE

Plant, Cell & Environment   PCE   WILEY

Tradeoffs between leaf cooling and hydraulic safety in a dominant arid land riparian tree species

Davis E. Blasini[1] | Dan F. Koepke[2] | Susan E. Bush[2] | Gerard J. Allan[3,4] |
Catherine A. Gehring[3,4] | Thomas G. Whitham[3,4] | Thomas A. Day[1] |
Kevin R. Hultine[2]

[1]School of Life Sciences, Arizona State University, Tempe, Arizona, USA

[2]Department of Research, Conservation and Collections, Desert Botanical Garden, Phoenix, Arizona, USA

[3]Center for Adaptable Western Landscapes, Northern Arizona University, Flagstaff, Arizona, USA

[4]Department of Biological Sciences, Northern Arizona University, Flagstaff, Arizona, USA

Correspondence
Davis E. Blasini, School of Life Sciences, Arizona State University, Tempe, AZ 85281, USA.
Email: dblasini@asu.edu

Abstract

Leaf carbon gain optimization in hot environments requires balancing leaf thermoregulation with avoiding excessive water loss via transpiration and hydraulic failure. The tradeoffs between leaf thermoregulation and transpirational water loss can determine the ecological consequences of heat waves that are increasing in frequency and intensity. We evaluated leaf thermoregulation strategies in warm- (>40°C maximum summer temperature) and cool-adapted (<40°C maximum summer temperature) genotypes of the foundation tree species, *Populus fremontii*, using a common garden near the mid-elevational point of its distribution. We measured leaf temperatures and assessed three modes of leaf thermoregulation: leaf morphology, midday canopy stomatal conductance and stomatal sensitivity to vapour pressure deficit. Data were used to parameterize a leaf energy balance model to estimate contrasts in midday leaf temperature in warm- and cool-adapted genotypes. Warm-adapted genotypes had 39% smaller leaves and 38% higher midday stomatal conductance, reflecting a 3.8°C cooler mean leaf temperature than cool-adapted genotypes. Leaf temperatures modelled over the warmest months were on average 1.1°C cooler in warm- relative to cool-adapted genotypes. Results show that plants adapted to warm environments are predisposed to tightly regulate leaf temperatures during heat waves, potentially at an increased risk of hydraulic failure.

KEYWORDS
arid land riparian ecosystem, experimental common garden, Fremont cottonwood, leaf economic traits, leaf temperature, stem sap flux, stomatal conductance

1 | INTRODUCTION

Leaf energy budgets are governed in part by the absorbance of incoming solar radiation and exchange of latent and sensible heat energy (Fauset et al., 2018; Lambers et al., 2008; Michaletz et al., 2015). Environmental conditions within plant canopies such as sunlight, air temperature, humidity and wind speed influence leaf radiant heating and heat transfer between leaves and the surrounding microclimate (Gutschick, 2016; Jones, 2014; Michaletz et al., 2016). Leaf size and conductance to water vapour alter leaf temperature by governing thickness of leaf boundary layers and how much heat loss occurs through sensible and latent heat flux per unit surface area (Dong et al., 2017; Leigh et al., 2017; Michaletz et al., 2016). However, the extent to which plants in natural environments are adapted to regulate leaf temperature in response to thermal stress is largely unknown.

Leaf carbon budgets are tightly coupled to leaf energy budgets because increases in leaf temperature (T_{leaf}) (see Table 1 for definitions and abbreviations) above an optimal temperature reduces

TABLE 1 List of abbreviations with common units

Abbreviation	Definition	Units
Meteorological variables		
vpd	Vapour pressure deficit	kPa
u	Open air wind speed	m s^{-1}
u_c	Canopy wind speed	m s^{-1}
u_v	Canopy frictional velocity	m s^{-1}
d	Zero plane displacement	m
z_m	Roughness length	m
d_l	Characteristic leaf dimension	m
Fluxes and conductance		
J_s	Sap flux density	g m^{-2} s^{-1}
G_c	Canopy conductance	mmol m^{-2} s^{-1} kPa
G_s	Canopy stomatal conductance	mmol m^{-2} s^{-1} kPa
G_{bl}	Boundary layer conductance	mmol m^{-2} s^{-1} kPa
G_r	Long-wave radiative transfer conductance	mmol m^{-2} s^{-1} kPa
γ	Psychrometric constant	kPa K^{-1}
λ	Latent heat of vaporization	J kg^{-1}
ρ	Density of moist air	kg m^{-3}
C_p	Specific heat of air	J kg^{-1} K^{-1}
e	Change in latent per change in sensible heat	Dimensionless
Ω	Canopy decoupling coefficient	Dimensionless
E	Whole-tree transpiration rate	g m^{-2} s^{-1}
G_{smax}	Theoretical maximum stomatal conductance	mmol m^{-2} s^{-1}
T_{air}	Air temperature	°C
T_{leaf}	Leaf temperature	°C
ΔT	Leaf-to-air temperature differences	°C
Plant measurements and allometry		
S_l	Leaf size	cm^2
A_l	Leaf area	m^2
A_s	Sapwood area	cm^2
H	Tree height	m
SLA	Specific leaf area	cm^2 g
D_{stom}	Stomatal density	#Stomata mm^2
S_{stom}	Stomatal size	μm^2

photosynthetic rates while increasing rates of respiration (Teskey et al., 2015). Likewise, leaf temperature affects the solubility of CO_2 in the liquid phase, kinetics of Rubisco, electron transport efficiency, and mesophyll conductance (Cen & Sage, 2005; Lambers et al., 2008;

Yamori et al., 2006). In particular, high leaf temperatures increase rates of photorespiration and subsequently negatively affect net photosynthesis (Atkin et al., 2006; Berry & Bjorkman, 1980; Lambers et al., 2008; Wahid et al., 2007). Exposure to extreme heat waves can also damage photosynthetic processes as high temperatures disrupt cell membranes and metabolism (Hazel, 1995). Therefore, traits that facilitate the maintenance of leaf temperatures close to the optima for photosynthesis should be highly favoured by selection (Helliker & Richter, 2008; Michaletz et al., 2015; 2016; Slot & Winter, 2016).

Leaves exhibiting morpho-physiological traits that modify thermal fluxes can display substantial differences between T_{leaf} and air temperature (T_{air}) (Blasini et al., 2020; Leigh et al., 2017; Michaletz et al., 2015; 2016). Leaf size, width, shape, orientation, reflectance and stomatal density can all modify T_{leaf} relative to T_{air} (Beerling et al., 2001; Leigh et al., 2017; Michaletz et al., 2015; O'sullivan et al., 2017; Wright et al., 2017). For example, under hot air temperature and high irradiance conditions, larger leaves are particularly susceptible to experience damaging leaf temperatures because they form thicker boundary layers that slow sensible and latent heat loss (Farquhar & Sharkey, 1982; Lambers et al., 2008; Martin et al., 1999; Wright et al., 2017). Consequently, larger leaves (i.e., large surface area) tend to display larger leaf-to-air temperature differences than smaller leaves (Leigh et al., 2017; Wright et al., 2017). On the other hand, because the high latent heat vaporization of water, stomatal regulation and subsequent leaf evaporative cooling caused by transpiration is arguably the most effective mechanism for regulating leaf temperature in extreme hot environments (Curtis et al., 2012; Drake et al., 2018; Hetherington & Woodward, 2003; Radin et al., 1994; Upchurch & Mahan, 1988). Recent evidence suggests that some plant taxa adapted to extreme hot environments display an alternative water-use strategy that prioritizes leaf evaporative cooling over immediate returns on water loss in the form of carbon acquisition (Aparecido et al., 2020; Urban et al., 2017). However, an inevitable tradeoff with maintaining high transpiration rates in hot and dry conditions runs the risk of operating with leaf water potentials at or near the turgor loss point and hydraulic failure. Thus, fine-tuning stomatal regulation of leaf water potential to balance midday leaf cooling with hydraulic failure avoidance may be a critically important trait in heat-adapted plants.

Here, we examine stomatal regulation of leaf water potential relative to midday leaf cooling in *Populus fremontii*, *Sarg.* (Fremont cottonwood), an obligate riparian phreatophytic tree species that inhabits arid regions in the southwest United States and northern Mexico. This species is an ideal candidate for studying genotypic variation in traits related to leaf thermoregulation because it is found across extremely broad elevational (0–2000 m.a.s.l) and climate gradients that encompass subfreezing to extreme hot temperatures (>40°C). Recent common garden experiments have found that *P. fremontii* displays large intraspecific variation in productivity (Grady et al., 2011), phenology (Cooper et al., 2019), and functional trait coordination (Blasini et al., 2020) in relation to the mean annual temperature (MAT) transfer distance, defined as the MAT of the source population location subtracted from the common garden

location. Previous studies have identified three *P. fremontii* ecotypes with boundaries that largely reflect distinct geographic regions. These include the relatively warm Sonoran Desert region, the relatively cool Colorado Plateau region of Utah and northern Arizona, and the California Central Valley region with a climate that is intermediate between the other two regions (Ikeda et al., 2017). Previous studies have identified genotypes sourced from populations adapted to cooler temperatures in the Colorado Plateau region that display a distinct combination of shorter growing seasons (i.e., later leaf flush and earlier fall senescence) with more conservative trait expression, while warm-adapted genotypes from the Sonoran Desert region exhibit longer growing seasons with more acquisitive trait expression at multiorgan levels (Blasini et al., 2020; Cooper et al., 2019). Here we define genotypes from populations with higher mean maximum summer temperatures than the common garden location as a warm-adapted ecotype, and a cool-adapted ecotype as genotypes from populations at or below mean maximum summer temperatures in relation to the common garden location.

Climate projections predict that the North American region in which *P. fremontii* occurs will become warmer and more arid over the remainder of the century (Breshears et al., 2013; Garfin et al., 2013; Seager et al., 2014). During the first decade of the 21st century, the region experienced higher daily average temperatures and more recurrent heat waves than in the previous 100 years (Garfin et al., 2013). As a consequence of episodic drought and heatwaves, *P. fremontii* has experienced recent mortality surges across its geographical range (Whitham et al., 2020).

We examined the overarching hypothesis that genotypes from the warm-adapted ecotype prioritize leaf cooling over hydraulic safety compared to genotypes from the cool-adapted ecotype. To test this hypothesis, we measured leaf temperature, leaf morphology and sap-flux-scaled canopy transpiration (E) and stomatal conductance (G_s) in *P. fremontii* genotypes sourced from seven populations representing the warm- and cool-adapted ecotypes and growing together in a common garden located near the mid-point of the species climate distribution (Cooper et al., 2019; Hultine et al., 2020a). We evaluated three primary modes of canopy thermal regulation, involving adjustment in (1) maximum midday stomatal conductance, (2) stomatal sensitivity to leaf to air vapour pressure deficit (vpd) as a trait for maintaining evaporative cooling under thermal stress, and (3) leaf morphology including specific leaf area (SLA), leaf size, leaf width and stomatal size and density. The field data were used to parameterize a leaf energy balance model to predict how leaf morphology and stomatal conductance influence leaf temperature over a wide range of thermal conditions. This allowed us to test four inter-related subhypotheses: (1) genotypes sourced from the warm-adapted ecotype maintain cooler midday canopies under well-watered conditions than genotypes sourced from the cool-adapted ecotype in mid-summer. (2) Genotypes sourced from the warm-adapted ecotype produce smaller leaves with higher SLAs and higher maximum theoretical stomatal conductance (G_{smax}) based on stomatal density and size than genotypes sourced from the cool-adapted ecotype. (3) Genotypes sourced from the

warm-adapted ecotype maintains higher midday stomatal conductance than genotypes sourced from the cool-adapted ecotype to facilitate leaf cooling. (4) As a consequence of having higher maximum G_s, genotypes sourced from the warm-adapted ecotype operate with a lower midday leaf water potential (Ψ_{md}) over the summer than genotypes sourced from the cool-adapted ecotype. Results from this investigation help identify genotypes that are likely to best cope with increases in temperature and episodic heat waves that are predicted for the southwestern United States, and more broadly provide new insights into local adaptation to extreme thermal stress and subsequent tradeoffs associated with leaf thermal regulation in dominant woody taxa.

2 | MATERIALS AND METHODS

2.1 | Study site

An experimental common garden was established in October 2014 with 16 *P. fremontii* populations (~4100 propagated cuttings) that collectively represent the climatic and elevational range of the species (Cooper et al., 2019; Hultine et al., 2020a). The garden was located within the Agua Fria National Monument in central Arizona (34°15′34.42″ N; 112°03′29.39″ W; elevation 988 m) (Figure 1) and was established on a 1.2 Ha portion of former cropland next to the intermittently flowing Agua Fria River. During the winter of 2013–2014, cuttings were collected from a total of 12 genotypes per population. Genotypes were collected at least 20 m apart to avoid using clones within each population. The individual cuttings were treated with root hormone and potted in the Northern Arizona University greenhouse for 4 months. In the garden, 0.3 m tall saplings were planted 2 m apart from each other in a randomized block design with a total of four replicated blocks, each with 16 populations comprising 64 genotypes each. A drip irrigation system was used to water each tree with approximately 20 L, 2–3 times per week during the growing season.

From the original 16 populations established in the garden, we studied 7 populations with a total of 56 genotypes ($n = 8$ genotypes per population) representing the broadest possible range in MAT of the source populations, from 10.7 to 22.6°C, and an elevation gradient from 72 to 1940 m (Figure 1). In addition to the local Agua Fria National Monument population, three populations, respectively, from sites with higher and lower mean maximum summer temperatures than the common garden location were selected. The three populations from the lower Sonoran Desert were defined as a warm-adapted ecotype because the extreme mean maximum summer temperatures (>40°C) they experience at their source sites is above that of the common garden location (Figure 2). The three populations from higher elevation provenances in the Sonoran Desert and Colorado Plateau were sourced from locations with similar or lower mean maximum summer temperatures than the common garden location and therefore were categorized as a cool-adapted ecotype (Figure 2).
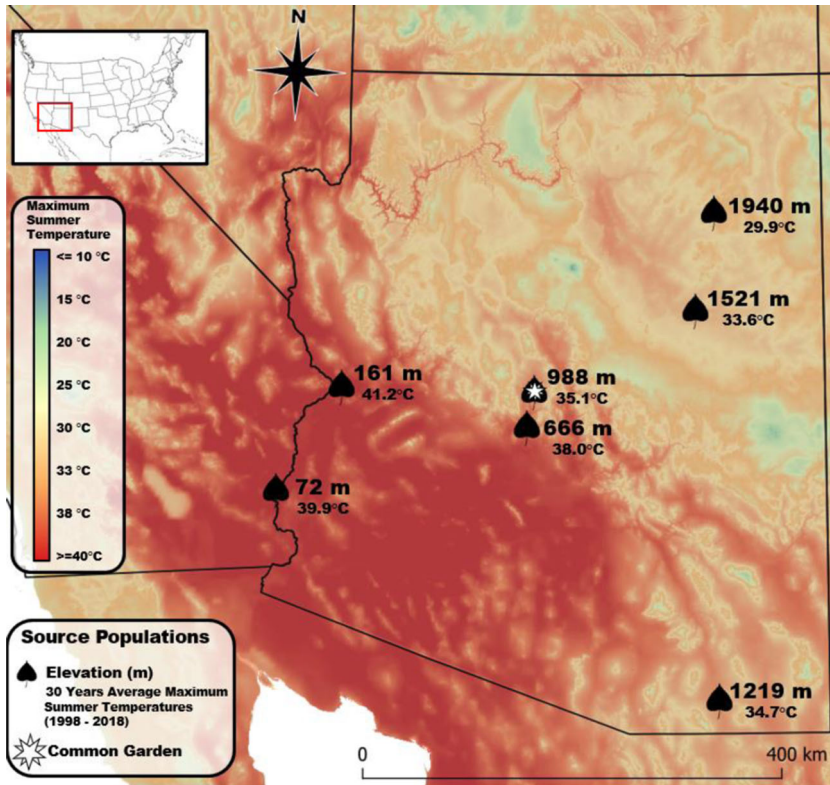
FIGURE 1 Location of the Agua Fria common garden (white star) and seven population sites of *Populus fremontii* (Fremont cottonwood leaf icon) with their 30-year maximum summer temperatures (Fick & Hijmans, 2017; QGIS Development Team, 2021) [Color figure can be viewed at wileyonlinelibrary.com]
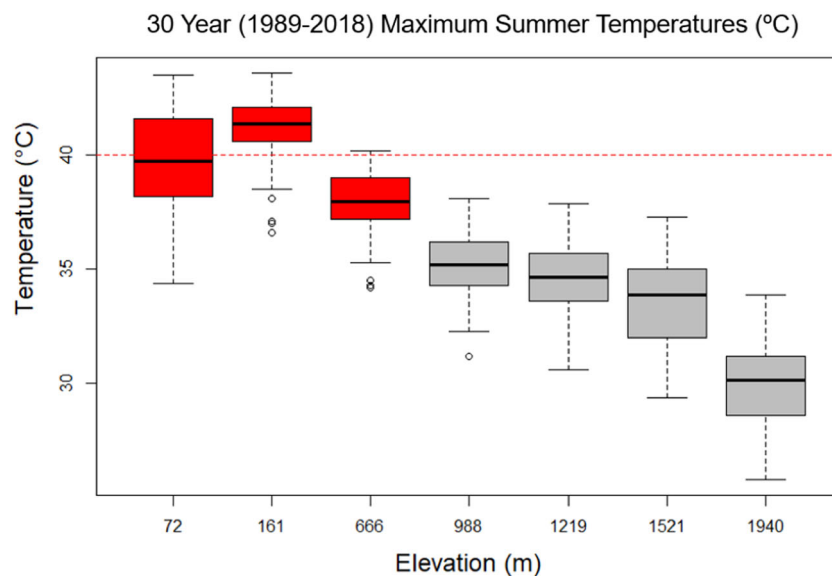

FIGURE 2 Box and whisker plots showing the median, 25th and 75th percentiles (boxes) and the 10th and 90th percentiles (error bars) of 30-year (1989–2018) maximum annual average summer temperatures grouped by the seven population sites of *Populus fremontii*. PRISM data (http://prism.oregonstate.edu). Red boxes represent populations adapted to mean maximum summer temperatures of >40°C (warm-adapted ecotypes) and grey boxes represent populations adapted to mean maximum summer temperatures of <40°C (cool-adapted ecotypes). Dotted red line represents 40°C maximum average summer temperatures [Color figure can be viewed at wileyonlinelibrary.com]

The experimental common garden and some of the genotypes used in this study were part of a previous investigation that studied morpho-physiological trait variability at multiple trait spectra in relation to local temperatures at the population source sites (Blasini et al., 2020). Results from Blasini et al. (2020) suggest trait expression in *P. fremontii* is highly coordinated and reflect local adaptation to either exposure to freeze–thaw conditions in high elevation populations or exposure to extreme thermal stress in low-elevation populations. In the present investigation, we evaluated intraspecific differences in leaf thermoregulation in relation with MAT and mean

maximum summer temperatures (MMST) transfer distances (Table 2), defined as the MAT and MMST of the source population location subtracted from the MAT and MMST of the common garden location (Grady et al., 2011).

2.2 | Meteorological data

A micrometeorological station installed at the garden measured relative humidity, air temperature, photosynthetically active radiation (Q, μmol m^{-2} s^{-1}) and wind speed continuously every 30 s and stored as 30 min means from 30 May (day 151) to 23 Oct (day 296) of 2017 with a Campbell CR10X-2M datalogger (Campbell Scientific). Air temperature and relative humidity were measured with a shielded Vaisala HMP 60 AC temperature/humidity probe (Vaisala) placed 3 m above the ground surface. Photosynthetic active radiation was measured with an Apogee SQ-110-SS sun calibration quantum Sensor (Apogee Instruments). We used air temperature and relative humidity to calculate air vapour pressure deficit (vpd, kPa) using both half-hourly and daily averages.

2.3 | Morphological traits

2.3.1 | Stomatal anatomy

In 2016, we randomly collected fully expanded leaves from mid-height and south-facing canopy of each genotype ($n = 56$) to determine stomatal density, length, width and area. We followed the nail polish impression method (Hilu & Randall, 1984) to obtain four impressions per leaf, two impressions in both the abaxial and adaxial sides of the leaves ($n = 560$ impressions). An Olympus CX41 light microscope (Olympus Corp.) was used to observe and obtain two images from each impression with a Moticam Pro 282A camera (Motic Instruments). Stomatal density (D_{stom}) was calculated as the number of stomata in eight (0.59 mm^2) digital images at 10× magnification per genotype. Stomatal size (S_{stom}) (length × width) was observed on 700 stomata from digital images at 40× magnification ($n = 100$ per population) using an open-source imaging programme, ImageJ (https://imagej.nih.gov/ij/). We calculated maximum theoretical stomatal conductance to water vapour (G_{smax}, mmol m^{-2} s^{-1}) following Franks and Farquhar (2001):

$$G_{\text{smax}} = \frac{d_{\text{w}} \cdot D_{\text{stom}} \cdot a_{\text{max}}}{v\left(1 + \frac{\pi}{2}\sqrt{\frac{a_{\text{max}}}{\pi}}\right)}, \tag{1}$$

where d_{w} is the diffusivity of water in air (2.43×10^{-5} m^2/s), v is the molar volume of air (0.024 m^3/mol; Jones, 2014), D_{stom} is the stomatal density, a_{max} is the maximum area of the open stomatal pore, approximated as $\pi(p/2)^2$, where p is stomatal pore length (μm), assumed to be stomatal length divided by two (Franks & Farquhar, 2007).

TABLE 2 Climatic variables of the seven provenances at the Agua Fria National Monument common garden

Ecoregion	Provenance elevation (m)	Latitude	Longitude	MAT (°C)	MMST (°C)	MAT (°C) transfer	MMST (°C) transfer	River flow regime	Annual average freezing days (1989–2018)	Stem area (cm²)	Whole-tree height H (m)
Cool-adapted	1940	35.8115	−110.18038	10.7	29.9	6.7	5.2	Intermittent	169	44.16 ± 4.52	3.15 ± 0.51
Cool-adapted	1521	34.9613	−110.38956	12.3	33.6	5.1	1.5	Intermittent	141	20.02 ± 1.65	2.44 ± 0.98
Cool-adapted	1212	31.4382	−110.76260	16.9	34.7	0.5	0.4	Perennial	58	43.79 ± 3.93	2.25 ± 0.40
Cool-adapted	988	34.2338	−111.04478	17.4	35.1	0.0	0.0	Intermittent	30	17.66 ± 1.26	2.25 ± 0.40
Warm-adapted	666	33.9540	−112.13526	19.9	38.0	−2.5	−2.9	Intermittent	6	41.78 ± 6.21	2.42 ± 0.68
Warm-adapted	161	34.2761	−114.05856	22.3	41.2	−4.9	−6.1	Intermittent	2	34.27 ± 4.48	1.83 ± 0.36
Warm-adapted	72	33.3621	−114.69856	22.6	39.9	−5.2	−4.8	Perennial	2	51.04 ± 6.39	2.03 ± 0.66

Note: Climatic characteristics include mean annual temperature (MAT), mean maximum summer temperature (MMST), mean annual precipitation (MAP), and 30-year annual average freezing days (1989–2018). Transfer distances for MAT (MAT of the garden minus MAT of the provenance) and MMST. The population 988 m is located near the common garden and thus has a transfer distance of zero. Results of mean ± SE ($n = 56$) comparison of whole-tree stem areas and heights in a common garden in central Arizona.

2.3.2 | Leaf traits

SLA (cm^2 g^{-1}) was calculated as the one-sided area of a fresh leaf, divided by its oven-dry mass (Wright & Westoby, 2002). SLA was measured in June, July and September 2017. A subset of 12–20 fully expanded leaves from the mid and south facing section of the canopy were collected per genotype and scanned with a high-resolution computer scanner, and one-sided leaf area was measured with Image J. The scanned leaves were then oven-dried for 72 h at 75°C and weighed to calculate SLA. Leaf size (S_l, cm^2) and leaf width (w_l, cm) were derived from the average leaf size from these measurements (Ackerly et al., 2002).

2.3.3 | Whole tree allometry

In July 2017, we used allometric relationships between whole-tree stem diameter and leaf area through a branch summation approach to estimate whole-tree canopy leaf area (A_l) and sapwood area (A_s). The diameter of all leaf-bearing branches from the main stem in each of the 56 genotypes were measured with a digital caliper. To calculate whole canopy leaf area, a subset of the collected leaves per genotype was scanned with a high-resolution computer scanner, and one-sided leaf area was measured with Image J. Then, we generated a regression of branch diameter to leaf area from a subset of branches per genotype. Scanned leaves were oven-dried for 72 h at 75°C within each subset of branches, and then their weight was multiplied by SLA to determine total leaf area of the branch (see Section 2.3.2). Whole-tree height (H), canopy diameters (4–8 measurements per genotype) and their respective canopy areas were measured five times during the 2017 growing season with a telescoping measuring pole. Canopy area (A_c) was determined using the ellipse equation, πab, where a is the mean radius of longest canopy axis and b is the radius of two perpendicular canopy axes (Ansley et al., 2012).

2.4 | Sap-flux-scaled canopy transpiration and stomatal conductance

We installed heat dissipation sensors (Granier, 1987) that measured stem sap flux density (J_s, g H$_2$O m^{-2} sapwood s^{-1}) on all 56 genotypes from June 2nd (day 153) to October 2nd (day 275) 2017. Each sensor consisted of a pair of 20 mm long, 2 mm diameter stainless steel probes inserted approximately 15 cm apart along the axis of the hydro-active xylem. The sap flux density was calculated from the differences in temperature between the heated and unheated reference probes. Sap flux density, J_s (g cm^{-2} s^{-1}), was calculated as

$$J_s = qk^p. \tag{2}$$

For diffuse porous tree species (e.g., *P. fremontii*), q is the prefactor coefficient (0.0119), p is the scaling exponent (1.23) and k is related to the temperature difference between the two probes (Bush et al., 2010; Granier, 1987):

$$k = \frac{\Delta T_0}{\Delta T} - 1, \tag{3}$$

where ΔT is the difference in temperature between the heated and unheated probes and ΔT_0 is the temperature difference during hydrostatic conditions (data provided in repository). We assumed that hydrostatic conditions only occurred during evening periods when vpd was at or near zero. Thus, in some cases a single value for ΔT_0 was used to calculate k over several days.

We calculated canopy transpiration (E, g m^{-2} s^{-1}) using the total sap flux density and sapwood area to leaf area ratio (A_s: A_l) according to:

$$E = J_s \cdot \frac{A_s}{A_l}. \tag{4}$$

From the sap flux measurements, we also calculated canopy conductance (G_c, mmol m^{-2} s^{-1}) using a simplified version of the Penman–Monteith equation (Campbell & Norman, 1998; Hultine et al., 2013; Monteith & Unsworth, 2013):

$$G_c = \frac{\gamma \cdot \lambda}{\rho \cdot c_p \cdot vpd} \cdot \frac{J_s \cdot A_s}{A_l}, \tag{5}$$

where A_s is the conducting sapwood area (m^2), A_l is the total leaf area (m^2), γ is the psychrometric constant (kPa K^{-1}), λ is the latent heat of vaporization (J kg^{-1}), ρ is the density of moist air (kg m^{-3}), and c_p is the specific heat of air at constant pressure (J kg^{-1} K^{-1}).

Internal bark diameter and the depth of hydro-active xylem was estimated to obtain A_s. Because of the young age of the trees (2.5 years), and because *Populus* trees tend to have large active sapwood depths with uniform sap velocities (Lambs & Muller, 2002), we assumed the active sapwood included the entire cross-sectional area beneath the bark. Measurements of leaf area index (LAI), the projected leaf area per unit of ground area (Bréda, 2003; Chapin et al., 2011; Watson, 1947), provided a way to estimate the physical boundaries between the whole-tree canopy and the surrounding atmosphere (Bréda, 2003). Therefore, whole tree leaf area (A_l) and canopy area (A_c) were used to calculate intraspecific differences in LAI and therefore canopy boundary layer resistances, where LAI is given by

$$LAI = \frac{A_l}{A_c}. \tag{6}$$

Canopy stomatal conductance (G_s) was extracted from measurements of G_c by evaluating leaf boundary layer conductance (G_{bl}; mmol m^{-2} s^{-1}), which can be small enough in broadleaf plants to decouple plant canopies from atmospheric conditions. We therefore calculated G_{bl} according to Jones (2014) to compare with calculated values of G_s (shown below):

$$G_{bl} = 306.7 \cdot \sqrt{\frac{u_c}{d_l}}, \tag{7}$$

where (d_l) is the mean leaf characteristic dimension calculated for each genotype ($d_l = 0.72 \times$ leaf width) and (u_c) is the mean canopy wind speed (Campbell & Norman, 1998; Jones, 2014). Mean

μ_c (m s^{-1}) was estimated from wind speed (μ) measured at 3 m above the ground level and by multiplying canopy frictional velocity (μ_v) to $\mu \cdot \mu_v$ was calculated following Campbell and Norman (1998) as

$$\mu_v = \frac{\mu \cdot 0.4}{\ln \frac{z-d}{z_m}}, \tag{8}$$

where z is the genotype canopy height (m), d is the zero-plane displacement (m), z_m is the roughness length (m), and 0.4 is the von Karman constant. We used population specific values of G_c and G_{bl} to estimate canopy stomatal conductance:

$$G_s = \frac{1}{\frac{1}{G_c} - \frac{1}{G_{bl}}}. \tag{9}$$

We calculated a dimensionless decoupling coefficient (Ω) (Hultine et al., 2013; Martin, 1989) to evaluate the sensitivity of transpiration to changes in boundary layer conductance.

$$\Omega = \frac{\varepsilon + 2 + \frac{G_r}{G_{bl}}}{\varepsilon + 2 + \frac{G_{bl}+G_r}{G_s} + \frac{G_r}{G_{bl}}}, \tag{10}$$

where ε is the change of latent heat to the change in sensible heat of saturated air and G_r is the long-wave radiative transfer conductance. Ω is expected to reach its upper limit (1.0) as the influence of stomatal resistance over transpiration decline.

2.5 | Leaf water potentials

From June to September 2017, leaf water potentials (Ψ) were measured every month at predawn (Ψ_{pd}; 0300–0500 h local time) and midday (Ψ_{md}; 1100–1300 h) on each genotype that was instrumented with sap flux probes using the Scholander pressure chamber (PMS Instruments; Scholander et al., 1965; Turner, 1988). To take these measurements, a single shoot tip from each of the 56 genotypes was cut with a sharp razor blade at mid-height and south-facing canopy. Differences between Ψ_{pd} and Ψ_{md} ($\Delta\Psi$) were calculated for each genotype, population, and ecotype over each measurement period, to provide an index of the transpiration-induced changes in water potential gradients from the roots to the leaves.

2.6 | Leaf temperature

We measured leaf temperature on 17 warm- and 24 cool-adapted genotypes (total $n = 41$) instrumented with the sap flux probes in the common garden between 13:00 and 15:00 h of 28th August (day 240) and 1st September (day 244) of 2017: two of the warmest days during the study. We evaluated leaf temperature on three to four separate leaves in each individual genotype using a thermal imaging camera ThermaCam (Flir One, Flir Systems). This handheld device integrates a thermal and visual sensor of 80 × 60 and 1440 × 1080 pixels, respectively, to a smartphone, with a typical accuracy range of ±3°C or ±5% (https://www.flir.com/products/flir-one-gen-3/).

Leaf temperatures were taken 30 cm away from a full expanded leaf at three to four different locations in the canopy. Only leaves located in the middle (1.5–2.0 m) and sun-lit areas of each tree canopies were used to measure leaf temperature. This resulted in a total of 81 and 92 leaf temperature measurements for Day 240 and Day 244, respectively (total $n = 173$ measurements, 99 measurements for cool-adapted genotype and 74 for warm-adapted genotypes on both days). We used air temperature data collected from the on-site micrometeorological station to calculate the difference between air and leaf temperatures (ΔT).

2.7 | Statistical analysis and leaf energy balance modelling

All statistical analyses were conducted in R version 4.0.2 (R Development Core Team 2011). Before analysing the data, we examined whether each variable met the assumptions of normality and homogeneity of variance, using a Shapiro and Barlett test.

2.7.1 | Analysis of trait variation between cool- and warm-adapted ecotypes

Morphological trait comparisons between cool- and warm-adapted ecotypes, including all measurements of leaf morphology, leaf area to sapwood area ratios, and mean daily sap-flux-scaled canopy fluxes were conducted using a standard Student's t-test.

Because riparian tree species are found exclusively in places with abundant water available, stomatal conductance, and whole-tree water use in this species are intrinsically influenced by atmospheric characteristics like irradiance, atmospheric CO_2 concentrations, and atmospheric vapour pressure deficit (Landsberg et al., 2017). Specifically, increases in vpd have been found to correlate with decreases in stomatal conductance while the stomatal sensitivity to changes in vpd has been described to be proportional to the stomatal conductance at low vpd levels (<1 kPa). This sensitivity of stomatal conductance to changes in vpd can be estimated from (Domec et al., 2009; Hultine et al., 2013; Oren et al., 1999):

$$G_s = G_{sref} - m \cdot (\ln \text{vpd}), \tag{11}$$

where G_{sref} is the value of G_s at vpd = 1 kPa in a log-linear relationship and m (the slope of the regression fit) describes the sensitivity of G_s to changes in vpd (i.e., ln vpd). We also calculated stomatal sensitivity standardized by G_{sref}^- (S) according to Oren et al. (1999) as $-m$ G_{sref}^{-1}. Regression analyses was used to investigate the relationships between G_s and $G_s{:}G_{sref}$ of the cool- and warm-adapted ecotypes to log(vpd) during the hottest time of the day (11:00 to 19:00). Comparisons in mean G_s and $G_s{:}G_{sref}$ between ecotypes in response to log (vpd) and the interaction ecotype*log(vpd) were analysed using analysis of covariance (ANCOVA).

Differences in Ψ_{pd}, Ψ_{md} and $\Delta\Psi$ between cool- and warm-adapted genotypes were analysed by individual mixed-effects repeated measures ANOVA (type III with Satterthwaite's method) using the 'lmer' R package (Bates et al., 2015; Kuznetsova et al., 2017). In this test, individual traits were represented as response variables while the group (cool- and warm-adapted ecotypes) and month were treated as categorical fixed effects with two and three levels, respectively. Individual genotype nested within ecotypes was incorporated as a random effect.

2.7.2 | Leaf energy budget model parameterization

A leaf energy balance model was executed in R (R Core Team, 2018) through the "tealeaves" package (Muir, 2019). The model calculates leaf temperature from a suite of leaf traits, environmental parameters, and physical constants. Leaf traits included leaf size, stomatal ratio (stomata density adaxial:stomatal density abaxial), and mean canopy stomatal conductance during the hottest time of the day (11:00 to 19:00) from 2nd June (Day 153) to 2nd October (day 275) 2017 were included in the model. The environmental parameters used in the model included air temperature, relative humidity and wind speed collected at the common garden during the hottest time of the day from 2nd June (day 153) to 2nd October (day 275) 2017. Other environmental parameters included in the model were atmospheric pressure at 998 m above sea level (90.0 kPa), reflectance for short-wave irradiance (albedo) (0.2, unitless) and incident short-wave (solar) radiation flux density (1000 W/m^2) (Muir, 2019; Okajima et al., 2012).

A sensitivity analysis was performed on three and two environmental and morphophysiological variables, respectively, to determine their overall effect on leaf temperature resulted from the leaf energy balance model. These variables were air temperature, relative humidity, wind speed (environmental) and stomatal conductance and leaf size (morphophysiological). We used the 'konfound' package in R to run the sensitivity analysis (Frank et al., 2013) to determine the influence that environmental variables (relative humidity, wind speed and air temperature) and morphophysiological traits (leaf size and stomatal conductance) have on the modelled leaf temperatures in *P. fremontii*.

2.7.3 | Analysis of trait variation among populations

We performed a principal component analysis (PCA) to analyse the relationship between seven morphophysiological traits (S_l, A_s:A_l, D_{stom}, G_s, Ψ_{md}, SLA and S_{stom}) and ΔT at the population level using the 'factoextra' and 'FactoMineR' packages (Kassambara & Mundt, 2017; Lê et al., 2008). We determined the number of meaningful PCA axes using the Kaiser criterion and the Broken Stick Model in the 'vegan' and 'biodiversity' R package. Trait representation in the principal component biplot was based on the magnitude of the correlation between each trait and the principal component. Thus, traits in this biplot were represented as vectors with a length and direction indicating the strength and trend of a given trait's relationship among other traits. Specific location of the vector in the biplot indicates the positive or negative impact that a trait has on each of the two components x-axis, first component (PC1) and y-axis, second component (PC2). To analyse the relationship between the seven populations and the traits distribution in the PCA biplot, we constructed seven 95% confidence ellipses based on the PCA scores of each population. Subsequently, we performed ANOVA Tukey's HSD tests to assess significant differences in PC axes scores at the population level.

3 | RESULTS

3.1 | Leaf traits and leaf temperature

As hypothesized, under well-watered conditions, the warm-adapted ecotype displayed cooler midday leaf temperatures than the cool-adapted ecotype during the hottest time of the day (13:00 to 15:00). Average leaf temperature in the warm-adapted ecotype was 2.80°C below the common garden ambient temperature while the cool-adapted ecotype exhibited a mean leaf temperature of 0.98°C above air temperature ($t = 3.84$, df = 50, $p < 0.001$) (Figure 3a and Table 3). The warm-adapted ecotype displayed 39% smaller leaves ($t = 4.15$, df = 68, $p < 0.001$) (Figure 3b) with 35% greater stomatal densities ($t = -5.95$, df = 67.39, $p < 0.001$) (Figure 3c) and 13% higher SLA ($t = 2.85$, df = 40, $p < 0.01$, Table 3) than the cool-adapted ecotype. Additionally, the warm-adapted ecotype exhibited 28% narrower leaves ($t = -4.68$, df = 66, $p < 0.001$) with shorter 17% stomata ($t = 6.56$, df = 53.09, $p < 0.001$) and slightly greater (8%) maximum theoretical stomatal conductance (G_{smax}) than the cool-adapted ecotype (Table 3).

3.2 | Sap-flux-scaled canopy transpiration and stomatal conductance

Mean J_s measured over the growing season was largely similar between warm- versus cool-adapted ecotypes until about mid-August (~Day 230) after which J_s was on average 12% higher in the warm-adapted ecotype (Figure S1). Mean J_s varied dramatically over the course of the growing season from less than 5 g m^{-2} s^{-1} to over 60 g m^{-2} s^{-1} depending on vapour pressure deficit (Figure S1) and photosynthetic active radiation (Q, data not shown). The warm-adapted ecotype displayed a 36% greater A_s:A_l than the cool-adapted ecotype ($t = 9.92$, df = 54, $p < 0.001$) (Figure 3d and Table 3). As a consequence, the warm-adapted ecotype exhibited 42.2% higher mean afternoon transpiration rates per unit leaf area ($t = -7.49$, df = 199.2, $p < 0.001$) over the course of the growing season, with contrasts between ecotypes becoming particularly large starting in mid-August around Day 230 (Figure 4a).

Similarly, the warm-adapted ecotype exhibited 38.8% higher canopy conductance (G_c) than the cool-adapted ecotype (Table 3). We found that cool and warm-adapted ecotypes displayed their lowest canopy stomatal conductance values of the season (2.57 and 3.03 mmol m^{-2} s^{-1}, respectively) on 19 June (Day 170), the day with the second highest recorded afternoon vpd (7.33 kPa) during the season (Figure 4b). On the other
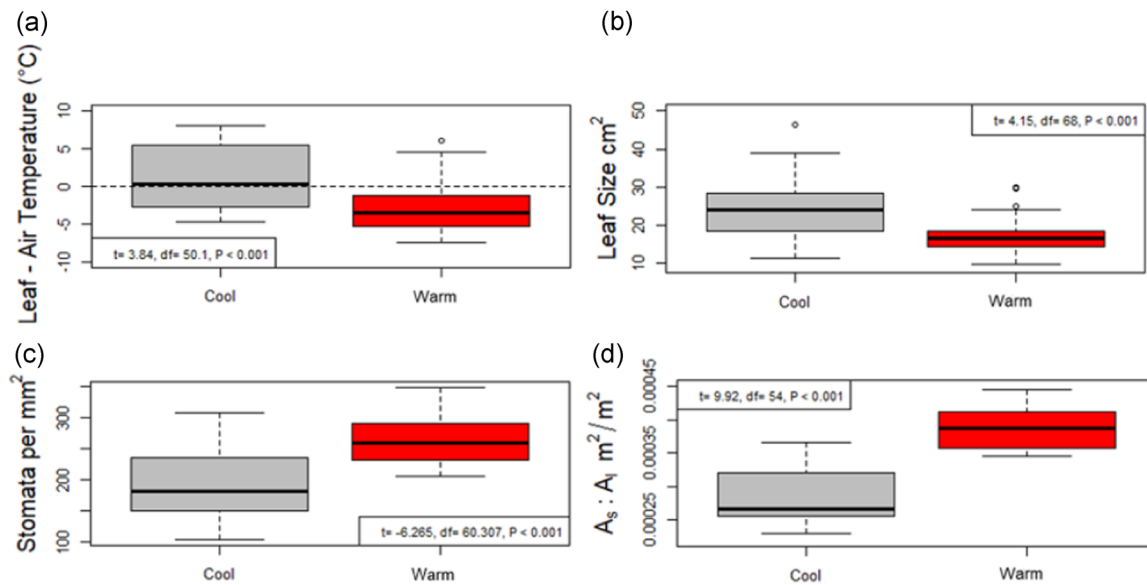
FIGURE 3 Multipanel box and whisker plots showing the median, 25th and 75th percentiles (boxes) and the 10th and 90th percentiles (error bars) of difference between the air and leaf temperatures (a), leaf size (b), stomatal density (c) and sapwood to leaf area ratio (d) of *Populus fremontii* genotypes occurring in a common garden in central Arizona. Internal legends indicate the *t*-value (*t*), degree of freedom (df) and *p* value (*p*) of the relationship between cool- and warm-adapted ecotypes. Warm-adapted genotypes (ecotype) were sourced from cuttings of mature *P. fremontii* trees occurring along the species warmest edge of its thermal distribution (*n* = 24 genotypes). Cool-adapted genotypes (ecotype) was sourced from cuttings of mature *P. fremontii* trees occurring along the species colder edge of its thermal distribution (*n* = 32 genotypes) [Color figure can be viewed at wileyonlinelibrary.com]

TABLE 3 Results of mean ± standard error and percent difference (*n* = 56) comparison of *Populus fremontii* functional traits between warm- and cool-adapted genotypes in a common garden in central Arizona

Trait	Cool	Warm	Percent difference
Leaf size (cm^2)	24.16 (±1.27)	17.27 (±0.97)	40%
Leaf width (cm)	5.98 (±0.20)	4.68 (±0.19)	28%
Specific leaf area (cm^2 g)	107.18 (±3.43)	121.26 (±3.41)	13%
Stomatal density (stomata mm^{-2})	194.61 (±9.11)	263.54 (±7.12)	35%
Stomata length (μm)	2.17e−05 (±4.4e−07)	1.86e−05 (±2.0e−07)	17%
Sapwood to leaf area (cm m^{-1})	0.029 (±7.4e−04)	0.039−(±6.7e−04)	36%
Transpiration (g m^{-2} s^{-1})	0.47 (±0.01)	0.67 (±0.02)	42.2%
Canopy conductance (mmol m^{-2} s^{-1})	14.4 (±0.70)	20.0 (±1.09)	38.8%
Canopy stomatal conductance (mmol m^{-2} s^{-1})	14.8 (±1.16)	20.4 (±1.64)	37.8%
Leaf temperature–air temperature (°C)	0.98 (±0.72)	−2.80 (±0.70)	3.8°C
Maximum theoretical stomatal conductance (mmol m^{-2} s^{-1})	1.12 (±0.18)	1.21 (±0.24)	8%

hand, both cool- and warm-adapted ecotypes displayed their greatest G_c values (50.5 and 69.5 mmol m^{-2} s^{-1}, respectively) on the day with the lowest vpd (1.35 kPa) recorded in the season (Day 205, July 24) (Figure 4b).

Canopies of both warm- and cool-adapted ecotypes were well coupled to the atmosphere such that the mean canopy decoupling coefficient was never higher than 0.05 for either group (Table 4). Therefore, cool- and warm-adapted ecotypes displayed G_s values that mirrored G_c. The warm-adapted ecotype exhibited 37.8% higher whole-season G_s (20.4 mmol m^{-2} s^{-1}) than the cool-adapted ecotype (14.8 mmol m^{-2} s^{-1}) (Table 4). Log-scale vpd explained 53% (F = 136.7, $p < 0.0001$) and 62% (F = 198.4, $p < 0.0001$) of the variation in mean daytime G_s of warm- and cool-adapted ecotypes, respectively (Figure 5a). Analysis of covariance revealed that across both ecotypes, G_s was highly correlated with vpd (F = 294.9, $p < 0.0001$). Increases in vpd resulted in decreases in G_s (Figure 5a). However, the relationship between G_s and
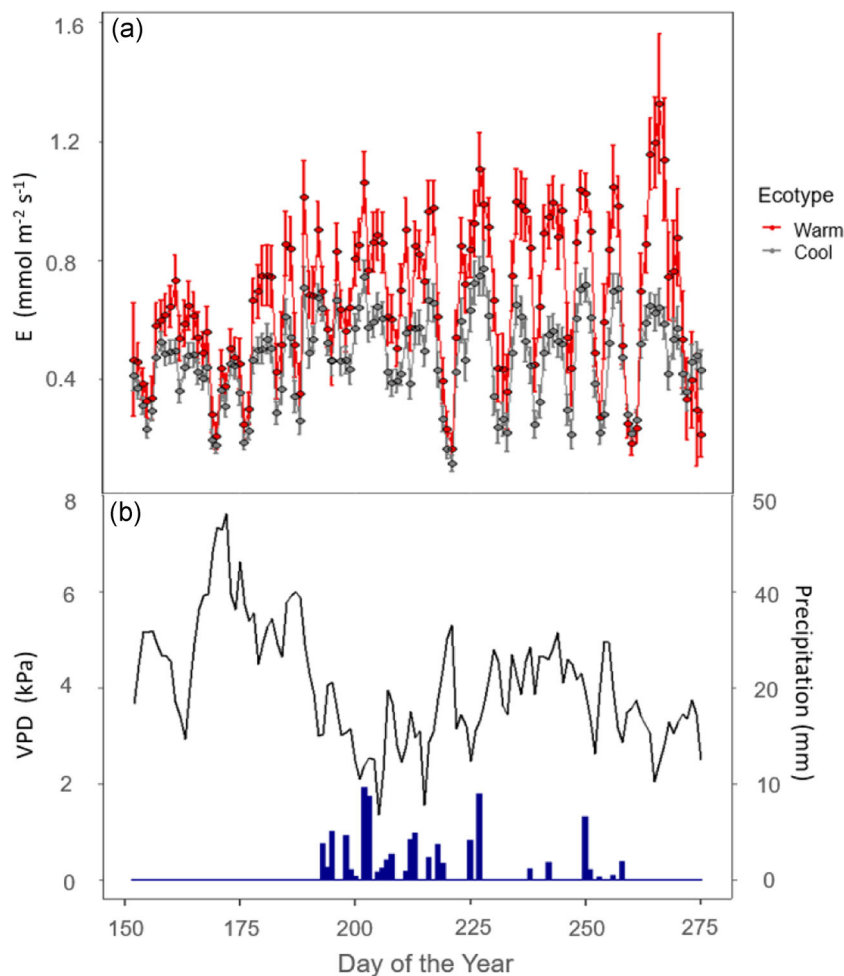
FIGURE 4 (a) Mean daily sap-flux scaled transpiration (E) measured between the hours of 1100 to 1900 from day of year 158 (June 7th) to day of year 275 (2 October) of the 2017 growing season on 24 warm-adapted genotypes and 32 cool -adapted genotypes occurring in a common garden in central Arizona. Error bars represent the standard errors of the mean. Warm-adapted genotypes (ecotype) were sourced from cuttings of mature *P. fremontii* trees occurring along the species warmest edge of its thermal distribution (*n* = 24 genotypes). Cool-adapted genotypes (ecotype) was sourced from cuttings of mature *P. fremontii* trees occurring along the species colder edge of its thermal distribution (*n* = 32 genotypes). (b) Mean daytime vapour pressure deficit (vpd) values calculated from measurements of local air temperature and relative humidity and precipitation values of the area of the garden obtained at PRISM data (http://prism.oregonstate.edu) [Color figure can be viewed at wileyonlinelibrary.com]

vpd differed between warm- and cool-adapted ecotypes ($F = 46.9$, $p < 0.0001$). The interaction between vpd and ecotypes was significant ($F = 9.40$, $p < 0.01$), as mean G_s converged at higher vpd values (Figure 5a).

There was a strong correlation between $G_s:G_{sref}$ and vpd in both warm- ($R^2 = 0.53$, $F = 2222$, $p < 0.0001$) and cool-adapted ($R^2 = 0.58$, $F = 2733$, $p < 0.0001$) ecotypes (Figure 5b). At the reference value of vpd = 1 kPa, reference G_s (i.e., G_{sref}) was 59% higher in the warm-adapted ecotype relative to the cool-adapted ecotype (66.3 mmol m^{-2} s^{-1} vs. 41.7 mmol m^{-2} s^{-1}, Figure 5a). However, the slope (m) that relates G_s with vpd was also 62% higher in warm-adapted ecotype than cool-adapted ecotype (−71.1 vs. 46.5 mmol m^{-2} s^{-1}, Figure 5a). Thus, stomatal sensitivity (S) to vpd was nearly equal between cool- (1.10 ± 0.020) and warm-adapted ecotypes (1.12 ± 0.029) (Figure 5b).

3.3 | Leaf water potentials

Predawn water potentials (Ψ_{pd}) ranged from −0.30 to −0.70 MPa throughout the growing season, indicating the trees were

TABLE 4 Results of mean ± standard error (*n* = 56) comparison of afternoon canopy stomatal conductance, afternoon stomatal conductance, and decoupling coefficient between warm- and cool-adapted ecotypes in a common garden in central Arizona

Ecotypes	Gc (mmol m^{-2} s^{-1})	Gs (mmol m^{-2} s^{-1})	Decoupling coefficient
Warm	20.0 (±1.55)	20.4 (±1.64)	0.047 (±0.002)
Cool	14.4 (±1.10)	14.8 (±1.16)	0.048 (±0.003)

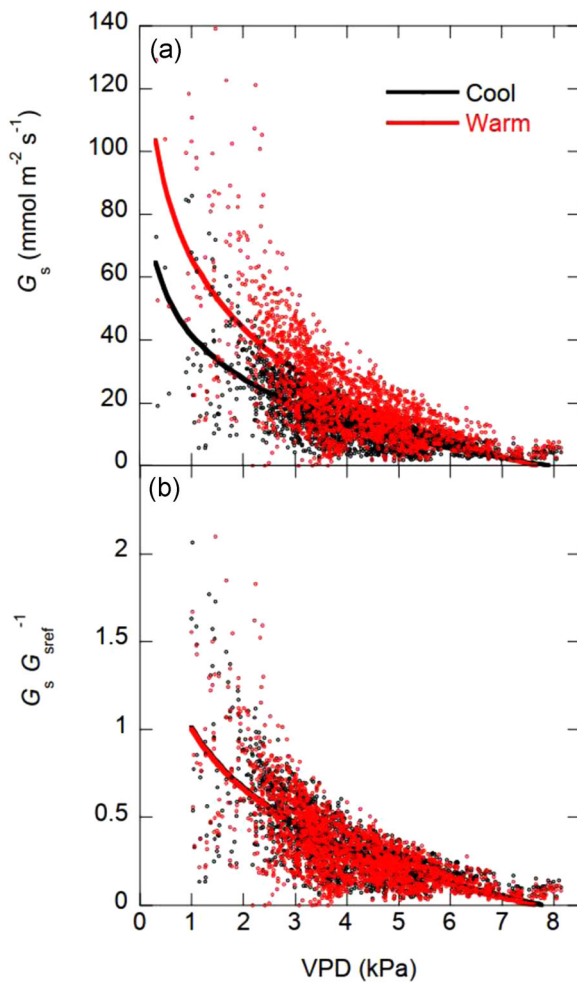| Population (m)	Gc	Gs	Decoupling coefficient
72	20.0 (±1.20)	20.6 (±1.25)	0.052 (±0.005)
161	14.2 (±4.43)	14.4 (±1.79)	0.034 (±0.004)
666	25.3 (±7.93)	26.1 (±3.38)	0.055 (±0.007)
988	16.4 (±3.00)	17.0 (±3.25)	0.047 (±0.008)
1212	12.7 (±3.49)	12.9 (±3.59)	0.064 (±0.004)
1521	10.3 (±1.12)	10.6 (±0.50)	0.037 (±0.002)
1940	18.1 (±5.65)	18.6 (±2.51)	0.044 (±0.006)

FIGURE 5 (A) Relationship between mean daily canopy stomatal conductance per unit leaf area (G_s) and mean daytime vapour pressure deficit (vpd) in warm- and cool-adapted *Populus fremontii* ecotypes at an experimental common garden in central Arizona. Data were collected between 11:00 and 19:00 from day of year 158 (7 June) to day of year 275 (2 October) of the 2017 growing season. (b) Stomatal conductance of warm- and cool-adapted ecotypes, normalized by a reference G_s (G_{sref}), defined at vpd = 1 kPa for data from day of year 158 to day of year 275 of the 2017 growing season [Color figure can be viewed at wileyonlinelibrary.com]

relatively well-watered, with the exception of occasional brief periods between irrigation events. We did not find significant differences in Ψ_{pd} between warm- and cool-adapted ecotypes (Figure 6a). However, the warm-adapted ecotype operated with lower mid-day leaf water potentials (Ψ_{md}) than the cool-adapted ecotype throughout the summer ($F = 11.63$, df = 1, $p < 0.01$, Figure 6b and Table S1), supporting hypothesis 4. Differences were most pronounced later in the growing season paralleling increased differences in canopy E between ecotypes (i.e., Figure 4a). Specifically, differences in Ψ_{md} between cool- and warm-adapted ecotypes were less than 0.1 MPa on Days 157 and 180, but increased to 0.23 MPa ($t = 3.15$, df = 40, $p < 0.01$) and 0.33 MPa

($t = 3.36$, df = 40, $p < 0.01$) on Days 208 and 236, respectively, with mean Ψ_{md} in the warm-adapted ecotype falling below −2.0 MPa on Day 236 (Figure 6b). As a consequence of progressive differences in Ψ_{md}, differences in ΔΨ between ecotypes also increased over the growing season (Figure 6c).

3.4 | Leaf energy balance model

Leaf temperature derived from the 'tealeaves' leaf energy balance model predicted leaves from the cool-adapted ecotype to be consistently hotter than the warm-adapted ecotype under identical air temperature scenarios (Figure 7). The average of all modelled leaf temperatures was 1.09°C hotter in the cool-adapted ecotype than the warm-adapted ecotype. Differences in leaf temperature between ecotypes were largely independent of air temperature, reflecting the similarity in stomatal sensitivity to vpd between ecotypes (Figure 5b). Sensitivity analysis showed that of the five variables explored (air temperature, relative humidity, wind speed, stomatal conductance and leaf size), air temperature had the greatest effect on modelled leaf temperatures (Figure S2a). However, when air temperature was held at a fixed value, leaf temperature was constrained primarily by canopy stomatal conductance (Figure S2b).

3.5 | Relationship between morpho-physiological traits and ΔT at the population level

To estimate the collective influence that multiple morpho-physiological traits have on the difference in leaf temperature between the cool- and warm-adapted ecotypes, we conducted a principal component analysis with seven morpho-physiological traits and leaf temperature. According to the Kaiser criterion and the Broken-Stick Model (Borcard et al., 2011), only the first principal component significantly explained the variance of the seven morpho-physiological traits and ΔT. This principal component (PC1) accounted for 56.7% of the variance and showed a significant positive relationship with S_l, ΔT, Ψ_{md} and S_{stom} while showing a negative significant correlation with A_s:A_l, D_{stom}, G_s and SLA. ANOVA and Tukey's HSD tests on population-level PC1 scores detected four significant different groups among the seven populations included in this study (Figures 8 and S3). Specifically, the two highest elevation populations with the most positive MAT and MMST transfer distances formed their own group (Group "a"), while the third highest elevation population (elevation 1219 m) was its own group (Group "b"). Interestingly, Group "c" was made up of three populations, the two lowest elevation populations with the most negative MAT and MMST transfer distances and the local population of the garden (elevation, 988 m). The last Group "d" was formed by the third lowest elevation population (elevation, 666 m) and the lowest elevation population which was also found in Group "c".
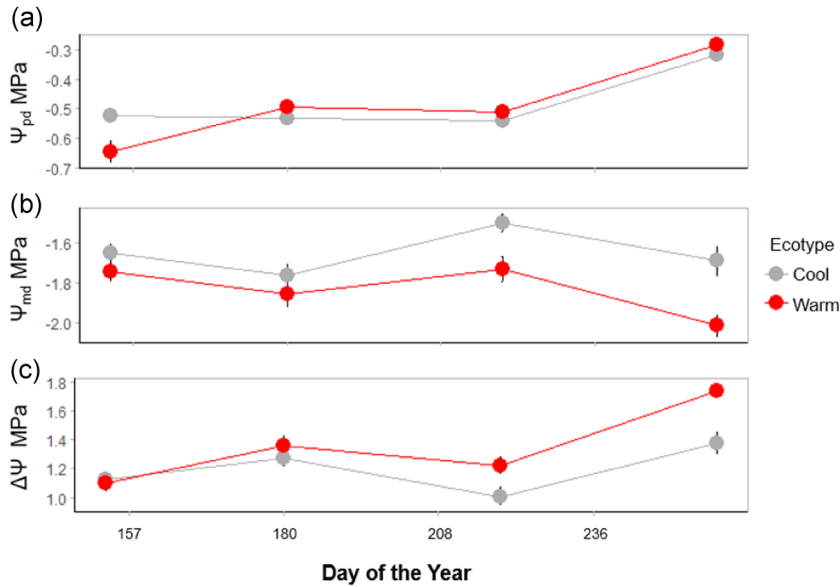
FIGURE 6 Mean predawn Ψ_{pd} (a), mid-day Ψ_{md} (b) and the difference between predawn Ψ_{pd} and mid-day Ψ_{md} ($\Delta\Psi$) (c) measured during four periods of the 2017 growing season on 24 warm-adapted genotypes and 32 cool-adapted *Populus fremontii* genotypes in a common garden located in central Arizona. Error bars represent the standard errors of the mean [Color figure can be viewed at wileyonlinelibrary.com]
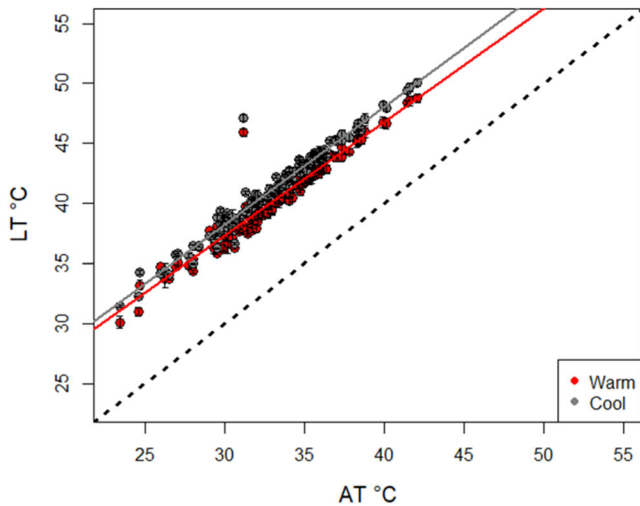

FIGURE 7 Relationship between energy balance estimations of leaf temperature and air temperature of warm- and cool-adapted *Populus fremontii* ecotypes. Estimates were modelled from measurements of leaf morphology, stomatal conductance, air temperature, relative humidity and wind speed (see Figure S3). Dash-black line indicates the 1:1 relationship between air temperature and leaf temperature [Color figure can be viewed at wileyonlinelibrary.com]

4 | DISCUSSION

We examined the overarching hypothesis that warm-adapted genotypes of the foundation tree species *P. fremontii* prioritize leaf cooling over hydraulic safety compared to cool-adapted genotypes. Using an experimental common garden, we assessed whether warm-adapted genotypes maintained cooler mid-summer leaf temperatures than cool-adapted genotypes and whether cooler leaf temperatures were correlated with a higher mean midday stomatal conductance, smaller

leaf size or both. Mid-summer, mid-afternoon leaf temperatures of genotypes sourced from the warm-adapted ecotype were on average 3.8°C cooler than genotypes from the cool-adapted ecotype, supporting our first subhypothesis. Contrasts in leaf temperatures between these two ecotypes corresponded with contrasts in leaf morphological traits including leaf size, leaf width, SLA and stomatal density, supporting our second subhypothesis. Genotypes of the warm-adapted ecotype also expressed a higher mean stomatal canopy conductance and associated transpiration rates, supporting our third subhypothesis, although stomatal sensitivity to vpd (S) was similar between the two ecotypes. Finally, the higher stomatal conductance in warm-adapted ecotype was coupled with lower mid-day leaf water potentials (Ψ_{md}) compared to the cool-adapted ecotype, supporting our fourth subhypothesis. Taken together, these results indicate that the warm-adapted ecotype maintains cooler mid-summer leaf temperatures that may be critical for maintaining leaf carbon budgets and avoiding leaf thermal damage under a warming climate in the southwestern US. However, increased leaf thermal regulation in the warm-adapted ecotype appears to correspond with enhanced hydraulic "risk taking" that could result in greater susceptibility to water deficits that are also predicted to increase in frequency and intensity in the southwest in the near future.

4.1 | Significance of leaf temperature

Genotypes on the warm edge of *P. fremontii's* distribution experience some of the most extreme summer heat waves in North America. Cooler leaf temperatures exhibited by genotypes sourced from the warm-adapted ecotype likely reflect extreme selection pressures to cope with chronic thermal stress that may be induced by air temperatures that often approach 50°C. To optimize canopy thermal regulation, the warm-adapted ecotype displayed a suite of morpho-physiological traits and hydraulic strategies that simultaneously

FIGURE 8 Relationship among the seven source populations elevation with principal component 1 loadings from a PCA using seven morpho-physiological traits (S_l, A_s:A_l, D_{stom}, G_s, Ψ_{md}, SLA and S_{stom}) and leaf-to-air temperature (ΔT) differences at the genotype level. Vertical bars represent standard error of the means (i.e., variation of genotypes within populations). Populations with different lowercase letters next to the data box and whisker indicate significant pairwise differences in PC1 scores using Tukey's HSD test
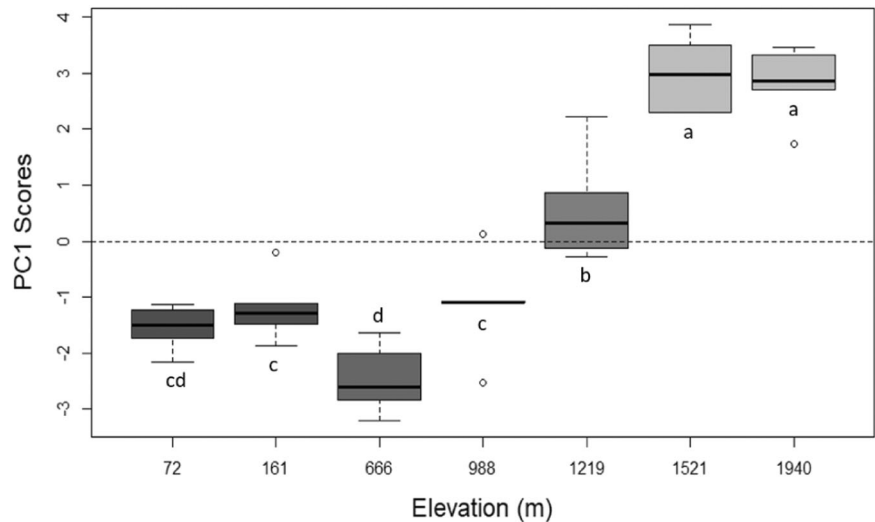
reduce leaf radiative load gain while increasing evaporative cooling. The combination of adaptive traits in the warm-adaptive ecotype is expected to reduce leaf photorespiration and maintenance respiration rates (Lloyd & Farquhar, 2008; O'Sullivan et al., 2013; Slot et al., 2016), while avoiding irreversible damage to chloroplasts and subsequently electron transport capacity of photosystem II (Kozaki & Takeba, 1996; Osmond & Björkman, 1972). The critical temperatures that affect photosystem II activity are generally species-specific or related to previous high-temperature exposure (Knight & Ackerly, 2003; O'sullivan et al., 2017; Teskey et al., 2015; Yordanov, 1992). However, high-temperature exposure has consistently been correlated with loss of chloroplast thermostability and decline of photosystem II quantum yield (Berry & Bjorkman, 1980; Hüve et al., 2011). Similarly, thylakoid membranes increase their fluidity, leakiness, and partial dissociation of light-harvesting complexes of photosystem II at extreme hot temperatures (Armond et al., 1980; Briantais et al., 1996; Hüve et al., 2011), underscoring the importance of leaf thermal regulation in hot environments.

Similar to field data collected from leaf thermal imagery, the 'tealeaves' leaf energy balance model predicted cooler leaf temperatures in the warm-adapted ecotype relative to the cool-adapted ecotype, under the same environmental conditions. However, the leaf energy balance model yielded a much smaller difference of 1.1°C instead of the 3.8°C found in our leaf thermal measurements. This difference could be explained by the fact that stomatal sensitivity to vpd was similar between ecotypes. According to the model, T_{leaf} was strongly governed by G_s (Figure S2b), and at relatively low vpd (i.e., vpd < 3 kPa), mean G_s of the warm-adapted ecotype was 55%–60% higher than the cool-adapted ecotype (Figure 5a). However, under warmer and drier conditions, G_s between ecotypes converged reflecting their similar sensitivities to vpd (Figure 5b). Therefore, differences in mid-summer, afternoon leaf temperatures detected by the model were largely a function of the cool-adapted ecotype having a larger and wider mean leaf size than the warm-adapted ecotype (Figure 3b), and not differences in evaporative cooling. Likewise, we cannot rule out an alternative hypothesis that

maintaining a higher midday stomatal conductance is not as much an adaptive trait for leaf cooling but more simply a necessity for warm-adapted plants to maintain photosynthesis and growth over the growing season. Nevertheless, given the 36% higher mean A_s:A_l (Figure 3d), and the equal to or higher mean J_s of the warm-adapted ecotype relative to the cool-adapted ecotype (Figure S1), it is highly plausible that afternoon leaf evaporative cooling was significantly more pronounced in the warm- versus cool-adapted ecotypes.

Minor changes in leaf temperature can have a significant impact of leaf carbon budgets because both mitochondrial respiration and photorespiration increase exponentially with tissue temperature (O'sullivan et al., 2017; Slot et al., 2016). For example, Q_{10} values (a proportional change in respiration with a 10°C increase in temperature) in the tissues of species in the genus *Populus* have been reported between 1.28 and 5.89 (Gielen et al., 2003; Griffin et al., 2001). Thus, a leaf temperature increases of just 1°C in these species would result in a 12.8%–58.9% increase in leaf respiration, although short-term (i.e., hours to days) thermal acclimation to warmer temperature could reduce plant Q_{10} values (Atkin & Tjoelker, 2003; Tjoelker et al., 2001). Likewise, photorespiration rates in C3 plants can increase substantially at leaf temperatures above 25°C, with a corresponding decrease in leaf carboxylation rates that can substantially reduce photosynthesis (Busch et al., 2013). Although the effect of higher temperatures on leaf photorespiration can vary by a species' optimum growth temperature (Cavanagh & Kubien, 2014; Galmés et al., 2016), photorespiration increases are generally related to the effect of high temperature on Rubisco specificity and the differences in solubility between CO_2 and O_2 (von Caemmerer & Quick, 2000).

4.2 | Hydraulic "risk taking" as an adaptive strategy to maintain cooler canopies

Intuitively, plants that maintain a relatively high stomatal conductance despite high atmospheric demand (e.g., high vpd) run the risk of steep declines in leaf turgor, xylem conductance or both, even when the

rhizosphere remains moist (Brodribb et al., 2017; Grossiord et al., 2020; Sperry et al., 2002). In the present study, Ψ_{md} was 0.3 MPa lower in the warm- relative to cool-adapted ecotypes by the end of the warm-season, corresponding with increased differences in G_s between ecotypes. For drought-intolerant species such as *P. fremontii*, small contrasts in Ψ_{md} may reflect important contrasts in plant water status between warm- and cool-adapted ecotypes. In fact, by late summer, mean Ψ_{md} in the warm-adapted ecotype fell below the xylem pressure (−1.88 MPa) at which near complete hydraulic failure has been reported to occur in *P. fremontii*—defined as the water potential that leads to 88% loss of xylem conductivity (Ψ_{88}: Choat et al., 2012). Conversely, mean Ψ_{md} in the cool-adapted ecotype never fell below −1.76, a level that is slightly above the reported threshold for hydraulic failure in *P. fremontii*. Whether contrasts in Ψ_{md} reflect differences in Ψ_{88} or other plant xylem traits among ecotypes is an open question, as previous studies have also reported midday water potentials in *P. fremontii* approaching −2.0 MPa (Leffler et al., 2000; Williams & Cooper, 2005). A similar study conducted at the same common garden as the present study reported that *P. fremontii* genotypes belonging to the relatively warm Sonoran Desert ecoregion had lower wood densities and xylem vessels with higher hydraulic mean diameters than genotypes sourced from the cooler Mogollon Rim ecoregion (Blasini et al., 2020): traits that could portend greater risk of hydraulic failure in the Sonoran Desert genotypes. In the present study, the warm-adapted ecotype had higher stomatal densities and a higher mean theoretical maximum stomatal conductance compared to the cool-adapted ecotype. Taken together, the lower Ψ_{md} values indicate that the warm-adapted ecotype may be adapted to operate with lower hydraulic safety margins to maintain cooler leaves. That, in turn, may limit the hydrological niche of the warm-adapted ecotype to locations with high perennial soil moisture availability (Hultine et al., 2020a).

Not surprisingly given their lower Ψ_{md} values, the reference midday G_s (i.e., G_{sref}) was almost 60% higher in the warm- versus cool-adapted ecotype. However, contrasts between ecotypes were not driven by differences in J_s, per se, but from the warm-adapted ecotype having a near 40% higher $A_s:A_l$. Leaf area to sapwood area ratios (the inverse of $A_s:A_l$) strongly decrease with aridity in angiosperm tree taxa (Gleason et al., 2013; Togashi et al., 2015). A relatively high $A_s:A_l$ can buffer plants from steep gradients in xylem water potential by maximizing the supply of water to individual leaves relative to demand that in turn can maximize leaf evaporative cooling under well-watered conditions. On the other hand, mean stomatal sensitivity to vpd was similar between ecotypes indicating that stomatal responses to atmospheric demand or dryness is a fixed trait among *P. fremontii* populations given similar exposure to soil water conditions.

4.3 | Adaptive trait syndromes at the population level

A primary advantage of common gardens in ecological studies is that they provide opportunities for potential evaluation of the coordination among traits—that is, adaptive trait syndromes—and resource fluxes within and among plants (Freschet et al., 2010; Reich, 2014).

For example, a previous study conducted on *P. fremontii* at the same common garden as the present study revealed that traits were not only coordinated across multiple organs and scales, but also identified two clearly defined adaptive trait syndromes (Blasini et al., 2020). Genotypes belonging to the relatively high-elevation Mogollon Rim ecoregion expressed a suite of conservative traits including spring leaf flush, leaf economic traits and wood economic traits relative to genotypes belonging to the lower elevation Sonoran Desert ecoregion (Blasini et al., 2020). Importantly, all five source populations that comprised the Sonoran Desert ecoregion shared similar mean trait values with one another, while all three populations that comprised the Mogollon Rim ecoregion also shared similar mean trait values with one another. These results indicate that all populations studied from the Sonoran Desert ecoregion shared a similar "acquisitive" adaptive trait syndrome that appeared to arise from selection to avoid leaf thermal damage (Blasini et al., 2020). Similarly, all populations from the Mogollon Rim ecoregion shared a similar "conservative" adaptive trait syndrome that appeared to arise from selection to avoid frost damage (Blasini et al., 2020).

In the present study, we defined a warm-adapted population as one where mean maximum summer temperature rose above 40°C. Indeed, results detected clear trait contrasts between the three warm-adapted populations, and the three coolest populations (Figure 8) that mirrored contrasts previously reported between the Sonoran Desert and Mogollon Rim ecoregions (Blasini et al., 2020). However, in contrast to our overarching hypothesis, genotypes from the mid-elevation population expressed traits that more closely paralleled genotypes sourced from the three warmest populations than the three cooler populations (Figure 8). One possible explanation is that selection pressures to cope with leaf thermal stress are expressed in genotypes from locations with lower mean maximum temperatures than 40°C. Alternatively, the mean trait expression of the mid-elevation population may reflect a certain "home field advantage" over genotypes from other locations given the 0°C transfer distance to the location of the common garden. Nevertheless, the clear adaptive trait syndromes identified here show that locally adapted *P. fremontii* populations may become maladapted under rapidly changing climate conditions across its geographical distribution.

5 | CONCLUSIONS

The resiliency of groundwater-dependent forest ecosystems to environmental change depends largely on resiliency of phreatophytic vegetation such as *P. fremontii* to alterations in groundwater availability coupled with rising temperatures. The dynamics of fluvial hydrology and groundwater availability undoubtedly act as strong agents of selection in *P. fremontii* in terms of hydraulic architecture, xylem anatomy and stomatal regulation (Blasini et al., 2020; Hultine et al., 2020a; 2020b). *P. fremontii* like other groundwater-dependent taxa in the southwestern United States occur in locations where groundwater is shallow enough for roots to maintain contact for most of the year. Shallow groundwater, therefore, allows *P. fremontii* trees to maximize productivity and resource uptake over

hydraulic safety. However, hydraulic "risk taking" may be amplified in *P. fremontii* ecotypes occurring on the warm edge of its distribution to cope with growing season temperatures that often approach 50°C. In the present study, warm-adapted genotypes, including those sourced along the extreme warm-edge of *P. fremontii's* distribution, displayed a higher maximum stomatal conductance and lower mid-day leaf water potentials that corresponded with lower daytime leaf temperatures than genotypes sourced from relatively cool locations. There is a growing body of evidence that some warm-adapted species forego hydraulic safety to optimize leaf temperature via transpirational cooling when exposed to hot conditions (Aparecido et al., 2020; Drake et al., 2018; Slot et al., 2016). Prioritizing leaf cooling over hydraulic safety would presumably limit the hydraulic niche of warm-adapted *P. fremontii* genotypes to locations where groundwater is not only shallow but is largely absent of daily or seasonal fluctuations that can temporarily decouple roots from the capillary fringe. Whether *P. fremontii* populations along the warm edge of its distribution can balance hydraulic safety with thermal regulation in the face of rapidly increasing aridity is an open question. Future investigations will need to couple physiology and genetics techniques to determine to what extent *P. fremontii* could overcome future extreme climatic conditions in the southwestern United States.

CONFLICT OF INTERESTS

The authors declare that there are no conflict of interests.

DATA AVAILABILITY STATEMENT

Data available from the Dryad Digital Repository https://doi.org/10.5061/dryad.hhmgqnkj9. (Blasini et al., 2022).

ORCID

Davis E. Blasini http://orcid.org/0000-0001-5005-9009
Gerard J. Allan http://orcid.org/0000-0002-8007-4784
Kevin R. Hultine http://orcid.org/0000-0001-9747-6037

REFERENCES

Ackerly, D., Knight, C., Weiss, S., Barton, K. & Starmer, K. (2002) Leaf size, specific leaf area and microhabitat distribution of chaparral woody plants: contrasting patterns in species level and community level analyses. *Oecologia*, 130, 449–457.

Ansley, R.J., Mirik, M., Surber, B.W. & Park, S.C. (2012) Canopy area and aboveground mass of individual Redberry Juniper (*Juniperus pinchotii*) trees. *Rangeland Ecology & Management*, 65, 189–195.

Aparecido, L.M.T., Woo, S., Suazo, C., Hultine, K.R. & Blonder, B. (2020) High water use in desert plants exposed to extreme heat. *Ecology Letters*, 23, 1189–1200.

Armond, U.A., Bjorkman, O. & Staehelin, L.A. (1980) Dissociation of supramolecular complexes in chloroplast membranes. A manifestation of heat damage to the photosynthetic apparatus. *Biochimica et Biophysica Acta*, 601, 433–442.

Atkin, O.K., Scheurwater, I. & Pons, T.L. (2006) High thermal acclimation potential of both photosynthesis and respiration in two lowland Plantago species in contrast to an alpine congeneric. *Global Change Biology*, 12, 500–515. Available at https://doi.org/10.1111/j.1365-2486.2006.01114.x

Atkin, O.K. & Tjoelker, M.G. (2003) Thermal acclimation and the dynamic response of plant respiration to temperature. *Trends in Plant Science*, 8, 343–351. Available at https://doi.org/10.1016/S1360-1385(03)00136-5

Bates, D., Mächler, M., Bolker, B. & Walker, S. (2015) Fitting linear mixed-effects models using lme4. *Journal of Statistical Software*, 67(1), 1–48. Available at https://doi.org/10.18637/jss.v067.i011

Beerling, D.J., Osborne, C.P. & Chaloner, W.G. (2001) Evolution of leaf-form in land plants linked to atmospheric CO_2 decline in the Late Palaeozoic era. *Nature*, 410, 352–354.

Berry, J. & Bjorkman, O. (1980) Photosynthetic response and adaptation to temperature in higher plants. *Annual Review of Plant Physiology*, 31, 491–543.

Blasini, D.E., Koepke, D.F., Grady, K.C., Allan, G.J., Gehring, C.A., Whitham, T.G. et al. (2020) Adaptive trait syndromes along multiple economic spectra define cold and warm adapted ecotypess in a widely distributed foundation tree species. *Journal of Ecology*, 109, 1298–1318.

Borcard, D., Gillet, F. & Legendre, P. (2011) *Numerical ecology with R*. Springer. Available at https://doi.org/10.1007/978-1-4419-7976-6

Bréda, N.J.J. (2003) Ground-based measurements of leaf area index: a review of methods, instruments and current controversies. *Journal of Experimental Botany*, 54, 2403–2417.

Breshears, D.D., Adams, H.D., Eamus, D., McDowell, N.G., Law, D.J., Will, R.E. et al. (2013) The critical amplifying role of increasing atmospheric moisture demand on tree mortality and associated regional die-off. *Frontiers in Plant Science*, 4, 264.

Briantais, J.M., Dacosta, J. & Goulas, Y. (1996) Heat stress induces in leaves an increase of the minimum level of chlorophyll fluorescence, Fo: a time-resolved analysis. *Photosynthesis Research*, 48, 189–196. Available at https://doi.org/10.1007/BF00041008

Brodribb, T.J., McAdam, S.A.M. & Carins Murphy, M.R. (2017) Xylem and stomata, coordinated through time and space. *Plant, Cell & Environment*, 40, 872–880. Available at https://doi.org/10.1111/pce.12817

Busch, F.A., Sage, T.L., Cousins, A.B. and Sage, R.F. (2013). C3 plants enhance rates of photosynthesis by reassimilating photo respired and respired CO2. *Plant, Cell & Environment* 36, 200-212. https://doi.org/10.1111/j.1365-3040.2012.02567.x

Bush, S.E., Hultine, K.R., Sperry, J.S., Ehleringer, J.R. & Phillips, N. (2010) Calibration of thermal dissipation sap flow probes for ring- and diffuse-porous trees. *Tree Physiology*, 30, 1545–1554.

Campbell, G. & Norman, J. (1998) *An introduction to environmental biophysics*, 2nd edition. Springer-Verlag.

Cavanagh, A.P. & Kubien, D.S. (2014) Can phenotypic plasticity in Rubisco performance contribute to photosynthetic acclimation? *Photosynthesis Research*, 119, 203-214.

Cen, Y.-P. & Sage, R.F. (2005) The regulation of Rubisco activity in response to variation in temperature and atmospheric CO_2 partial pressure in sweet potato. *Plant Physiology*, 139, 979–990.

Chapin, F.S., Matson, P.A. & Vitousek, P.M. (2011) *Principles of terrestrial ecosystem ecology*. Springer. Available at https://doi.org/10.1007/978-1-4419-9504-9

Choat, B., Jansen, S., Brodribb, T.J., Cochard, H., Delzon, S., Bhaskar, R. et al. (2012) Global convergence in the vulnerability of forests to drought. *Nature*, 491, 752–755. Available at https://doi.org/10.1038/nature11688

Cooper, H.F., Grady, K.C., Cowan, J.A., Best, R.J., Allan, G.J. & Whitham, T.G. (2019) Genotypic variation in phenological plasticity: reciprocal common gardens reveal adaptive responses to warmer springs but not to fall frost. *Global Change Biology*, 25, 187–200.

Curtis, E.M., Leigh, A. & Rayburg, S. (2012) Relationships among leaf traits of Australian arid zone plants: alternative modes of thermal protection. *Australian Journal of Botany*, 60, 471–483.

Domec, J.-C., Noormets, A., King, J.S., Sun, G., McNulty, S.G., Gavazzi, M.J. et al. (2009) Decoupling the influence of leaf and root hydraulic conductances on stomatal conductance and its sensitivity to vapour pressure deficit as a soil dries in a drained loblolly pine plantation. *Plant, Cell & Environment*, 32, 980–991. Available at https://doi.org/10.1111/j.1365-3040.2009.01981.x

Dong, N., Prentice, I.C., Harrison, S.P., Song, Q.H. & Zhang, Y.P. (2017) Biophysical homoeostasis of leaf temperature: a neglected process for vegetation and land-surface modelling. *Global Ecology and Biogeography*, 26, 998–1007.

Drake, J.E., Tjoelker, M.G., Vårhammar, A., Medlyn, B.E., Reich, P.B., Leigh, A. et al. (2018) Trees tolerate an extreme heatwave via sustained transpirational cooling and increased leaf thermal tolerance. *Global Change Biology*, 24, 2390–2402.

Farquhar, G.D. & Sharkey, T.D. (1982) Stomatal conductance and photosynthesis. *Annual Review of Plant Physiology*, 33, 317–345.

Fauset, S., Freitas, H.C., Galbraith, D.R., Sullivan, M.J.P., Aidar, M.P.M., Joly, C.A. et al. (2018) Differences in leaf thermoregulation and water use strategies between three co-occurring Atlantic forest tree species: leaf energy balance of Atlantic forest trees. *Plant, Cell & Environment*, 41, 1618–1631.

Fick, S.E. & Hijmans, R.J. (2017) Worldclim 2: new 1-km spatial resolution climate surfaces for global land areas. *International Journal of Climatology*, http://worldclim.org/version2

Frank, K.A., Maroulis, S.J., Duong, M.Q. & Kelcey, B.M. (2013) What would it take to change an inference? Using Rubin's causal model to interpret the robustness of causal inferences. *Educational Evaluation and Policy Analysis*, 35(4), 437–460. Available at https://doi.org/10.3102/0162373713493129

Franks, P.J. & Farquhar, G.D. (2001) The effect of exogenous abscisic acid on stomatal development, stomatal mechanics, and leaf gas exchange in Tradescantia virginiana. *Plant Physiology*, 125(2), 935–942. Available at https://doi.org/10.1104/pp.125.2.935

Franks, P.J. & Farquhar, G.D. (2007) The mechanical diversity of stomata and its significance in gas-exchange control. *Plant Physiology*, 143(1), 78–87. Available at https://doi.org/10.1104/pp.106.089367

Freschet, G.T., Cornelissen, J.H.C., van Logtestijn, R.S.P. & Aerts, R. (2010) Evidence of the 'plant economics spectrum' in a subarctic flora. *Journal of Ecology*, 98(2), 362–373. Available at https://doi.org/10.1111/j.1365-2745.2009.01615.x

Galmés, J., Hermida-Carrera, C., Laanisto, L. & Niinemets, Ü. (2016) A compendium of temperature responses of Rubisco kinetic traits: variability among and within photosynthetic groups and impacts on photosynthesis modeling. *Journal of Experimental Botany*, 67, 5067–5091.

Garfin, G., Jardine, A., Merideth, R., Black, M. & LeRoy, S. (Eds.) (2013) *Assessment of climate change in the southwest United States: a report prepared for the National Climate Assessment*. Island Press/Center for Resource Economics.

Gielen, B., Liberloo, M., Bogaert, J., Calfapietra, C., DeAngelis, P., Miglietta, F. et al. (2003) Three years of free-air CO_2 enrichment (POPFACE) only slightly affect profiles of light and leaf characteristics in closed canopies of Populus. *Global Change Biology*, 9, 1022–1037.

Gleason, S.M., Butler, D.W. & Waryszak, P. (2013) Shifts in leaf and stem hydraulictraits across aridity gradients in eastern Australia. *International Journal of Plant Sciences*, 174, 1292–130.

Grady, K.C., Ferrier, S.M., Kolb, T.E., Hart, S.C., Allan, G.J. & Whitham, T.G. (2011) Genetic variation in productivity of foundation riparian species at the edge of their distribution: implications for restoration and assisted migration in a warming climate. *Global Change Biology*, 17, 3724–3735.

Granier, A. (1987) Evaluation of transpiration in a Douglas-fir stand by means of sap flow measurements. *Tree Physiology*, 4, 309–320.

Griffin, K.L., Tissue, D.T., Turnbull, M.H., Schuster, W. & Whitehead, D. (2001) Leaf dark respiration as a function of canopy position in Nothofagus fusca trees grown at ambient and elevated CO_2 partial pressures for five years. *Functional Ecology*, 15, 497–505.

Grossiord, C., Buckley, T.N., Cernusak, L.A., Novick, K.A., Poulter, B., Siegwolf, R.T.W. et al. (2020) Plant responses to rising vapor pressure deficit. *New Phytologist*, 226, 1550–1566. Available at https://doi.org/10.1111/nph.16485

Gutschick, V.P. (2016) *Leaf energy balance: basics and modeling from leaves to canopies*. Springer Netherlands, pp. 23–58.

Hazel, J.R. (1995) Thermal adaptation in biological membranes: is homeoviscous adaptation the explanation? *Annual Review of Physiology*, 57, 19–42.

Helliker, B.R. & Richter, S.L. (2008) Subtropical to boreal convergence of tree-leaf temperatures. *Nature*, 454, 511–514.

Hetherington, A.M. & Woodward, F.I. (2003) The role of stomata in sensing and driving environmental change. *Nature*, 424, 901–908.

Hilu, K.W. & Randall, J.L. (1984) Convenient method for studying grass leaf epidermis. *Taxon*, 33(3), 413–415. Available at https://doi.org/10.2307/1220980

Hultine, K.R., Allan, G.J., Blasini, D., Bothwell, H.M., Cadmus, A., Cooper, H.F. et al. (2020a) Adaptive capacity in the foundation tree species Populus fremontii: implications for resilience to climate change and non-native species invasion in the American Southwest. *Conservation Physiology*, 8(1), coaa061.

Hultine, K.R., Burtch, K.G. & Ehleringer, J.R. (2013) Gender specific patterns of carbon uptake and water use in a dominant riparian tree species exposed to a warming climate. *Global Change Biology*, 19, 3390–3405.

Hultine, K.R., Froend, R., Blasini, D., Bush, S.E., Karlinski, M. & Koepke, D.F. (2020b) Hydraulic traits that buffer deep-rooted plants from changes in hydrology and climate. *Hydrological Processes*, 34(2), 209–222. Available at https://doi.org/10.1002/hyp.13587

Hüve, K., Bichelea, I., Ivanovab, H., Keerbergb, O., Parnik, T., Rasulova, B. et al. (2011) Temperature responses of dark respiration in relation to leaf sugar concentration. *Physiologia Plantarum*, 144(4), 320–34. Available at https://doi.org/10.1111/j.1399-3054.2011.01562.x

Ikeda, D.H., Max, T.L., Allan, G.J., Lau, M.K., Shuster, S.M. & Whitham, T.G. (2017) Genetically informed ecological niche models improve climate change predictions. *Global Change Biology*, 23, 164–176. Available at https://doi.org/10.1111/gcb.13470

Jones, H.G. (2014) *Plants and microclimate: a quantitative approach to environmental plant physiology*, 3rd edition. Cambridge University Press.

Kassambara, A. & Mundt, F. (2017). factoextra: extract and visualize the results of multivariate data analyses. *R package version 1.0.5*. https://CRAN.Rproject.org/package=factoextra.

Knight, C.A. & Ackerly, D.D. (2003) Evolution and plasticity of photosynthetic thermal tolerance, specific leaf area and leaf size: congeneric species from desert and coastal environments. *New Phytologist*, 160, 337–347.

Kozaki, A. & Takeba, G. (1996) Photorespiration protects C₃ plants from photooxidation. *Nature*. 384, 557–560.

Kuznetsova, A., Brockhoff, P.B. & Christensen, R.H.B. (2017) lmerTest package: tests in linear mixed effects models. *Journal of Statistical Software*, 82(13), 1–26. Available at https://doi.org/10.18637/jss.v082.i13

Lambers, H., Chapin, F.S. & Pons, T.L. (2008) *Plant Physiological Ecology*. Springer.

Lambs, L. & Muller, E. (2002) Sap flow and water transfer in the Garonne River riparian woodland, France: first results on poplar and willow. *Annals of Forest Science*, 59, 301–305. https://doi.org/10.1051/forest:2002026

Landsberg, J., Waring, R. & Ryan, M. (2017) Water relations in tree physiology: where to from here? *Tree Physiology*, 37(1), 18–32. Available at https://doi.org/10.1093/treephys/tpw102

Lê, S., Josse, J. & Husson, F. (2008) FactoMineR: an R package for multivariate analysis. *Journal of Statistical Software*, 25, 1–18. Available at https://doi.org/10.18637/jss.v025.i01

Leffler, A.J., England, L.E. & Naito, J. (2000) Vulnerability of Fremont cottonwood (*Populus fremontii*) individuals to xylem cavitation. *Western North American Naturalist*, 60, 204–210.

Leigh, A., Sevanto, S., Close, J.D. & Nicotra, A.B. (2017) The influence of leaf size and shape on leaf thermal dynamics: does theory hold up under natural conditions? *Plant, Cell & Environment*, 40, 237–248.

Lloyd, J. & Farquhar, G.D. (2008) Effects of rising temperatures and [CO₂] on the physiology of tropical forest trees. *Philosophical Transactions of the Royal Society of Britain*, 363, 1811–1817. Available at https://doi.org/10.1098/rstb.2007.0032

Martin, P. (1989) The significance of radiative coupling between vegetation and the atmosphere. *Agricultural and Forest Meteorology*, 49, 45–53.

Martin, T.A., Hinckley, T.M., Meinzer, F.C. & Sprugel, D.G. (1999) Boundary layer conductance, leaf temperature and transpiration of *Abies amabilis* branches. *Tree Physiology*, 19, 435–443.

Michaletz, S.T., Weiser, M.D., McDowell, N.G., Zhou, J., Kaspari, M., Helliker, B.R. et al. (2016) The energetic and carbon economic origins of leaf thermoregulation. *Nature Plants*, 2, 16129.

Michaletz, S.T., Weiser, M.D., Zhou, J., Kaspari, M., Helliker, B.R. & Enquist, B.J. (2015) Plant thermoregulation: energetics, trait-environment interactions, and carbon economics. *Trends in Ecology and Evolution*, 30, 714–724.

Monteith, J. & Unsworth, M. (2013) *Principles of environmental physics: plants, animals, and the atmosphere*, 4th edition. Elsevier, p. 400.

Muir, C.D. (2019) Tealeaves: an R package for modelling leaf temperature using energy budgets. *AoB Plants*, 11, 1–10.

Okajima, Y., Taneda, H., Noguchi, K. & Terashima, I. (2012) Optimum leaf size predicted by a novel leaf energy balance model incorporating dependencies of photosynthesis on light and temperature. *Ecological Research*, 27, 333–346.

Oren, R., Sperry, J.S., Katul, G., Pataki, D.E., Ewers, B.E., Phillips, N. et al. (1999) Survey and synthesis of intra- and interspecific variation in stomatal sensitivity to vapour pressure deficit. *Plant, Cell & Environment*, 22, 1515–1526.

Osmond, C.B. & Björkman, O. (1972) Simultaneous measurements of oxygen effects on net photosynthesis and glycolate metabolism in C3 and C4 species of Atriplex. *Carnegie Inst Wash Yearb*, 71, 141–148.

O'Sullivan, O.S., Weerasinghe, K.K., Evans, J.R., Egerton, J.J., Tjoelker, M.G. & Atkin, O.K. (2013) High-resolution temperature responses of leaf respiration in snow gum (*Eucalyptus pauciflora*) reveal high-temperature limits to respiratory function. *Plant Cell & Environment*, 36, 1268–1284.

O'sullivan, O.S., Heskel, M.A., Reich, P.B., Tjoelker, M.G., Weerasinghe, L.K., Penillard, A. et al. (2017) Thermal limits of leaf metabolism across biomes. *Global Change Biology*, 23, 209–223.

QGIS Development Team. (2021) *QGIS geographic information system*. Open-Source Geospatial Foundation Project. http://qgis.osgeo.org

Radin, J.W., Lu, Z., Percy, R.G. & Zeiger, E. (1994) Genetic variability for stomatal conductance in Pima cotton and its relation to improvements of heat adaptation. *Proceedings of the National Academy of Sciences*, 91, 7217–7221.

Reich, P.B. (2014) The world-wide 'fast–slow' plant economics spectrum: a traits manifesto. *Journal of Ecology*, 102(2), 275–301. Available at https://doi.org/10.1111/1365-2745.12211

Scholander, P.F., Hammel, H.T., Bradstreet, E.D. & Hemmingsen, E.A. (1965) Sap pressure in vascular plants. *Science*, 148, 339–346.

Seager, R., Goddard, L., Nakamura, J., Henderson, N. & Lee, D.E. (2014) Dynamical causes of the 2010/11 Texas–Northern Mexico drought. *Journal of Hydrometeorology*, 15, 39–68.

Slot, M. & Winter, K. (2016) The effects of rising temperature on the ecophysiology of tropical forest trees. In: Santiago, L.S. & Goldstein, G. (Eds.) *Tropical tree physiology*. Springer International Publishing, pp. 385–412.

Sperry, J.S., Hacke, U.G., Oren, R. & Comstock, J.P. (2002) Water deficits and hydraulic limits to leaf water supply. *Plant, Cell & Environment*, 25, 251–263. Available at https://doi.org/10.1046/j.0016-8025.2001.00799.x

Teskey, R., Wertin, T., Bauweraerts, I., Ameye, M., Mcguire, M.A. & Steppe, K. (2015) Responses of tree species to heat waves and extreme heat events: tree response to extreme heat. *Plant, Cell & Environment*, 38, 1699–1712.

Tjoelker, M., Olesksyn, J. & Reich, P. (2001) Modelling respiration of vegetation: evidence for a general temperature-dependent Q10. *Global Change Biology*, 7(2), 223–230. Available at https://doi.org/10.1046/j.1365-2486.2001.00397.x

Togashi, H.F., Prentice, I.C., Evans, B.J., Forrester, D.I., Drake, P., Feikema, P. et al. (2015) Morphological and moisture availability controls of the leaf area-to-sapwood area ratio: analysis of measurements on Australian trees. *Ecology and Evolution*, 5(6), 1263–1270.

Turner, N.C. (1988) Measurement of plant water status by the pressure chamber technique. *Irrigation Science*, 9, 289–308.

Upchurch, D.R. & Mahan, J.R. (1988) Maintenance of constant leaf temperature by plants—II. Experimental observations in cotton. *Environmental and Experimental Botany*, 28, 359–366.

Urban, J., Ingwers, M., McGuire, M.A. & Teskey, R.O. (2017) Stomatal conductance increases with rising temperature. *Plant Signaling & Behavior*, 12, 8. Available at https://doi.org/10.1080/15592324.2017.1356534

von Caemmerer, S. & Quick, W.P. (2000) Rubisco: physiology in vivoIn: Leegood, R.C., Sharkey, T.D. & Caemmerer, S. (Eds.) *Photosynthesis: physiology and metabolism*. Kluwer Academic Publishers, pp. 85–113. von Eds.

Wahid, A., Gelani, S., Ashraf, M. & Foolad, M.R. (2007) Heat tolerance in plants: an overview. *Environmental and Experimental Botany*, 61, 199–223. Available at https://doi.org/10.1016/j.envexpbot.2007.05.011

Watson, D.J. (1947) Comparative physiological studies on the growth of field crops. *Annals of Botany*, 11, 41–76.

Whitham, T.G., Gehring, C.A., Bothwell, H.M., Cooper, H.F., Allan, G.J. & Grady, K.C. et al. (2020) Using the Southwest experimental garden array to enhance riparian restoration in response to global environmental change: identifying and deploying genotypes and populations for current and future environments (Chapter 4). In: Carothers S.W., Johnson R.R., Finch D.M., Kingsley, K.J.,

Hamre, R.H., (Tech. Eds.) *Riparian research and management: past, present, future.* Volume 2. Gen. Tech. Rep. RMRS-GTR-411. Department of Agriculture, Forest Service, Rocky Mountain Research Station. pp. 63–79.

Williams, C.A. & Cooper, D.J. (2005) Mechanisms of riparian cottonwood decline along regulated rivers. *Ecosystems*, 8, 1–14.

Wright, I.J., Dong, N., Maire, V., Prentice, I.C., Westoby, M., Díaz, S. et al. (2017) Global climatic drivers of leaf size. *Plant Ecology*, 357, 917–920.

Wright, I.J. & Westoby, M. (2002) Leaves at low versus high rainfall: coordination of structure, lifespan and physiology. *New Phytologist*, 155(3), 403–416. Available at https://doi.org/10.1046/j.1469-8137.2002.00479.x

Yamori, W., Suzuki, K., Noguchi, K., Nakai, M. & Terashima, I. (2006) Effects of Rubisco kinetics and Rubisco activation state on the temperature dependence of the photosynthetic rate in spinach leaves from contrasting growth temperatures. *Plant, Cell & Environment*, 29, 1659–1670.

Yordanov, I. (1992) Response of photosynthetic apparatus to temperature stress and molecular mechanisms of its adaptations. *Photosynthetica*, 26(4), 517–531.

SUPPORTING INFORMATION

Additional supporting information may be found in the online version of the article at the publisher's website.